Aerosol effect on climate extremes in Europe under different future scenarios

J. Sillmann,[1] L. Pozzoli,[2] E. Vignati,[3] S. Kloster,[4] and J. Feichter[4]

Received 20 February 2013; revised 4 April 2013; accepted 8 April 2013; published 31 May 2013.

[1] This study investigates changes in extreme temperature and precipitation events under different future scenarios of anthropogenic aerosol emissions (i.e., SO_2 and black and organic carbon) simulated with an aerosol-climate model (ECHAM5-HAM) with focus on Europe. The simulations include a maximum feasible aerosol reduction (MFR) scenario and a current legislation emission (CLE_{mod}) scenario where Europe implements the MFR scenario, but the rest of the world follows the current legislation scenario and a greenhouse gas scenario. The strongest changes relative to the year 2000 are projected for the MFR scenario, in which the global aerosol reduction greatly enforces the general warming effect due to greenhouse gases and results in significant increases of temperature and precipitation extremes in Europe. Regional warming effects can also be identified from aerosol reductions under the CLE_{mod} scenario. This becomes most obvious in the increase of the hottest summer daytime temperatures in Northern Europe. **Citation:** Sillmann, J., L. Pozzoli, E. Vignati, S. Kloster, and J. Feichter (2013), Aerosol effect on climate extremes in Europe under different future scenarios, *Geophys. Res. Lett.*, *40*, 2290–2295, doi:10.1002/grl.50459.

1. Introduction

[2] Aerosols represent an important component of the climate system due to their direct effect on the radiative transfer budget and indirect effects through aerosol-cloud interactions. Although the direct and indirect effects of aerosol forcing constitute a large uncertainty in climate model simulations of the radiative forcing, state-of-the-art global climate models (GCMs) remain an essential tool for describing aerosol effects on the climate [e.g., *Forster et al*., 2007]. Depending on the type, aerosols can have significant cooling (e.g., sulfate) or warming (e.g., black carbon) effects on regional and global climate; thus, aerosols can amplify or dampen the impacts of anthropogenic climate change [e.g., *Ramanathan and Feng*, 2009; *Fiore et al*., 2012].

[3] As pointed out in the Special Report on Managing the Risks of Extreme Events (SREX) [*IPCC*, 2012], climate change is most perceived by society through the impacts of climate extremes, which often are associated with substantial economic and human losses. Climate extremes, such as extremely hot days, extreme precipitation, and longer dry spells, are projected to amplify under increased greenhouse gas concentrations as projected by large ensembles of GCMs [e.g., *Tebaldi et al*., 2006; *Orlowsky and Seneviratne*, 2012; *Sillmann et al*., 2013b]. Only few studies included the effect of aerosol emissions on the changes in climate extremes [e.g., *Caesar and Lowe*, 2012]. These changes will not be homogeneously distributed, depending on the regulations imposed by single countries or at the community level, such as the European Union.

[4] The objective of this study is to identify changes in climate extremes under future scenarios of anthropogenic aerosol emissions simulated with a global aerosol-climate model. We particularly focus on the effect of changes in anthropogenic sulfur dioxide (SO_2, the main precursor of sulfate aerosol) and black and organic carbon (BC and OC, respectively) emissions on temperature and precipitation extremes in Europe. We compare these climate extremes as simulated for present climate conditions with three scenarios for the year 2030: The first scenario (MFR) includes simulations of an aerosol emission scenario under maximum feasible aerosol reduction. In the second (CLE_{mod}), we investigate the impact of the world's aerosol emissions on Europe under the assumption that Europe implements the MFR scenario but the rest of the world follows a current legislation scenario. The last scenario (GHG) prescribes changes in greenhouse gas concentrations only and not in air pollutant emissions.

2. Methodology

2.1. Climate Model Simulations

[5] We use the ECHAM5-HAM fully coupled aerosol-climate model with a horizontal resolution of approximately $1.75° \times 1.75°$ and 31 vertical levels, from the surface up to 10 hPa. The model is composed of the general circulation model (GCM) ECHAM5 [*Roeckner et al.*, 2003] extended by the microphysical aerosol model HAM [*Stier et al.*, 2005] and coupled to a mixed-layer ocean [*Roeckner et al.*, 1995]. The sulfur chemistry is described by *Feichter et al.* [1996]. The aerosols, composed of sulfate (SO_4^{2-}), OC and BC, mineral dust, and sea salt are described by seven lognormal modes as in *Vignati et al.* [2004] and *Stier et al.* [2005].

Additional supporting information may be found in the online version of this article.

[1]Canadian Centre for Climate Modelling and Analysis, University of Victoria, Victoria, British Columbia, Canada.
[2]Eurasia Institute of Earth Sciences, Istanbul Technical University, Istanbul, Turkey.
[3]Joint Research Centre Institute for Environment and Sustainability, Climate Risk Management Unit, Ispra, Varese, Italy.
[4]Max Planck Institute for Meteorology, Hamburg, Germany.

Corresponding author: J. Sillmann, Canadian Centre for Climate Modelling and Analysis, University of Victoria, Victoria, BC, Canada. (jana.sillmann@ec.gc.ca)

0094-8276/13/10.1002/grl.50459

Table 1. Aerosol Experiments Considered in This Study[a]

	GHG Concentration	Aerosol Emissions	Oxidant Concentrations	Reference
CONTROL	2000	2000	2000	*Kloster et al.* [2010]
MFR	2030	2030 MFR	2030 MFR	*Kloster et al.* [2010]
CLE_{mod}	2030	2030 MFR Europe, CLE rest of the world	2030 MFR	*Kulmala et al.* [2011]
GHG	2030	2000	2000	*Kloster et al.* [2010]

[a]With the emission inventories, greenhouse gases, and oxidant concentrations as prescribed for the respective years.

2.1.1. Aerosol Experiments

[6] We consider a control simulation as well as three future climate scenarios in this study (cf. Table 1), which we describe in more detail below. Anthropogenic SO_2, BC, and OC emissions for present day (2000) and future scenarios for 2030 were developed by IIASA (International Institute for Applied System Analysis) [*Cofala et al*., 2007].

[7] The CONTROL experiment uses greenhouse gas and aerosol emissions as observed in year 2000 and is simulated for 100 years, but only 60 years after reaching the equilibrium are analyzed. The maximum feasible reduction (MFR) scenario assumes a worldwide implementation of the most advanced technologies available today to drastically reduce aerosol emissions. To study the influence of global emissions on Europe, we further include an aerosol experiment (CLE_{mod}), in which we make the assumption that Europe implements MFR measures in 2030 but the rest of the world follows the current legislation emission (CLE) scenario. The CLE scenario in general takes into account only presently decided control legislation for future developments and assumes a lower emission reduction than the MFR scenario. For Europe, differences in aerosol burdens are similar for BC and OC in MFR and CLE_{mod}, whereas the sulfate burden is decreasing much more in MFR (48–57%) than in CLE_{mod} (23–38%) (in the supporting information, see Tables S1 and S2, respectively, for total anthropogenic aerosol emissions and aerosol burdens over Europe). The greenhouse gas (GHG) experiment assumes only changes in greenhouse gas concentrations, and aerosol emissions are kept constant at the level of year 2000 [*Kloster et al*., 2010]. GHG concentrations are prescribed according to scenario B2 of the Special Report on Emission Scenarios (SRES) [*Nakicenovic et al*., 2000]. Natural emissions (dimethyl sulfide, sea salt, and dust) are simulated interactively in the model. Biomass burning emissions are assumed to be the same as for the year 2000. Changes in aerosol burdens over Europe for the three scenarios are illustrated in Figure S1 in the supporting information.

[8] Future scenario experiments include 60 years of simulations, but only the last 30 years were analyzed, in which the model is in an equilibrium state. For each scenario experiment, we performed three ensemble simulations to account for internal variability. More details on emissions, GHGs, and oxidant concentrations as well as calculations of the radiative forcing and mean climate impacts, particularly of MFR, are found in *Kloster et al.* [2010].

[9] The simulations used in this study are equilibrium climate experiments to specified emission and aerosol scenarios representing an equilibrium climate response to the prescribed forcing, which differs from a transient response. Thus, our results are based on simulations of 30 different years of the same climate forcing, which provides a robust statistic with regard to the forcing scenarios. Note that the simulations were preformed with a mixed-layer ocean and thus do not take into account fully coupled ocean feedback mechanisms.

2.2. Indices for Climate Extremes

[10] To capture climate extremes, we use a set of indices based on daily temperature and precipitation data as defined by the Expert Team for Climate Change Detection and Indices (ETCCDI) [e.g., *Zhang et al*., 2011]. These indices describe moderate extreme events, which can be reasonably well simulated by GCMs [e.g., *Sillmann et al*., 2013a]. In this study, we particularly focus on three temperature and precipitation indices, respectively, which are also discussed in more detail in *Sillmann and Roeckner* [2008] regarding their representation in the coupled atmosphere-ocean model ECHAM5/MPI-OM.

[11] The maximum of the daily maximum temperature (TXx) captures the hottest day of the year, which occurs in summer months, and the minimum of the minimum temperature (TNn) typically captures the coldest night of the year, which occurs in winter months. Tropical nights (TR) describe days with minimum temperatures above 20°C, thus indicating very hot nighttime conditions. Increases in this index, particularly in regions not well adapted to heat, can have considerable impacts on human health [e.g., *Patz et al*., 2005].

[12] Consecutive dry days (CDD) describe the maximum number of days with precipitation less than 1 mm and thus refers to the length of the longest dry spell per year. The maximum 5 day precipitation amount (RX5day) is often used to indicate extreme conditions that can lead to flooding events. Very wet days (R95p) describe the precipitation amount that falls on days with precipitation above the 95th percentile of the precipitation distribution in the base period (i.e., 30 years from CONTROL experiment).

3. Results

[13] In the following, we will focus on differences between present day (i.e., year 2000) and the three future scenarios for the year 2030 to illustrate the impact of future emissions on Europe. For every model grid cell, the 30 year median from the three future scenarios (MFR, CLE_{mod}, and GHG) was compared to the 60 year median from the CONTROL simulation (see Figure S2 in the supporting information for the 60 year climatology of the indices). The Wilcoxon signed rank test was used to verify that the 60 year CONTROL and 30 year future scenario data come from a continuous distribution symmetric about their median. Statistical significance of the median differences was measured by a two-tailed *t* test at 5% significance level. Only grid cells with statistically significant differences are displayed in Figures 1 and 2.

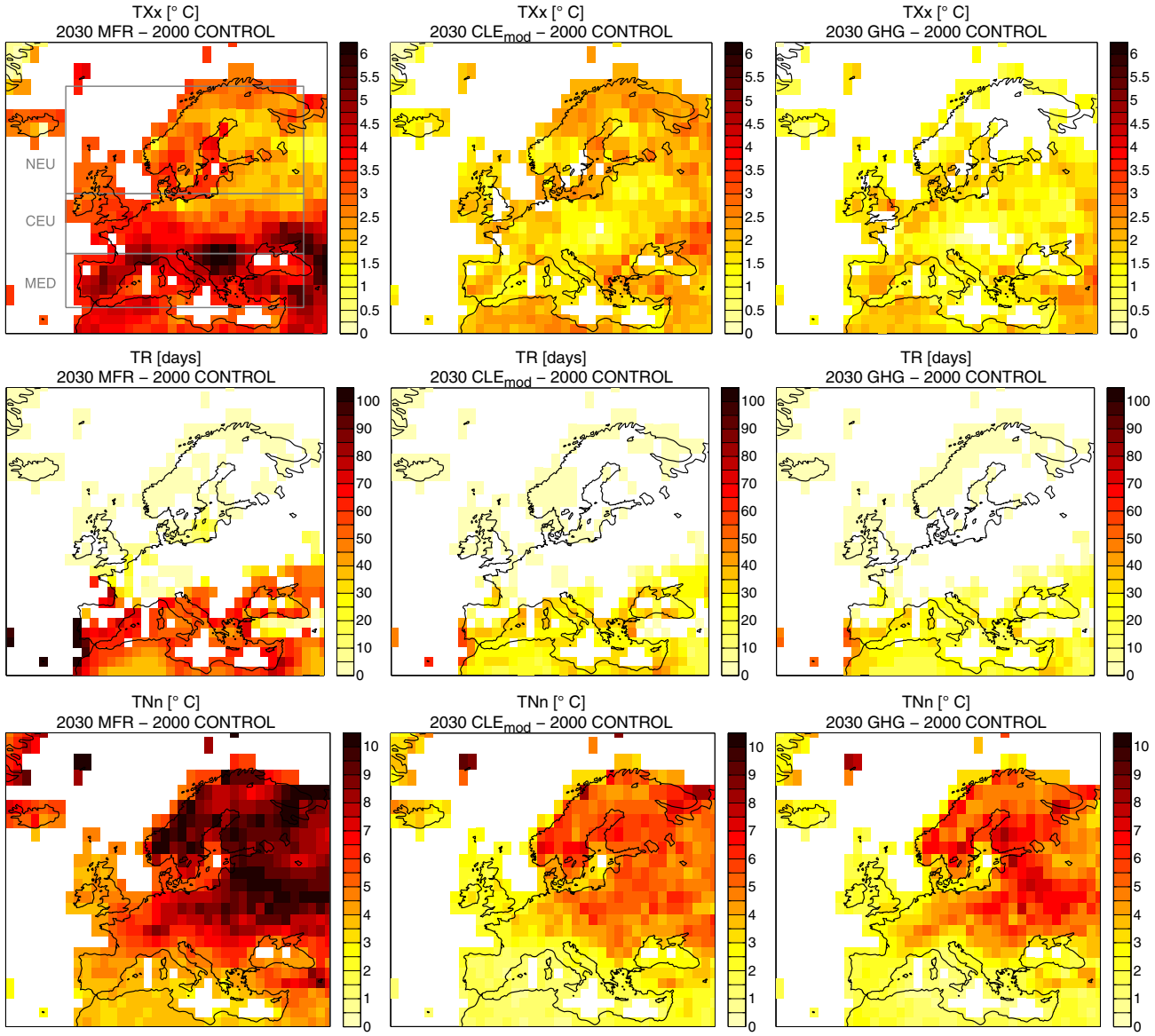

Figure 1. Changes in extreme temperature indices (TXx, TR, and TNn) due to the three future scenarios, maximum feasible reduction (MFR, left panels), MFR in Europe only and current legislation emission in the rest of the world (CLE$_{mod}$, middle panels), and GHG only emission scenario (GHG, right panels), compared to present climate conditions (CONTROL). Ocean grid cells and changes not statistically significant at the 5% significance level are not shown.

3.1. Spatial Patterns of Changes in Temperature and Precipitation Extremes

[14] A decrease in aerosol emissions worldwide prescribed by the MFR scenario compared to present-time climate will result in changing precipitation patterns and increasing temperatures everywhere in the world including Europe (see Figures 2c and 3 in *Kloster et al.*, [2010]).

[15] This is also represented in the significant increase of temperature extremes, as represented by TXx, TNn, and TR in Figure 1, which shows a stronger increase in MFR compared to the other scenarios CLE$_{mod}$ and GHG. The warming pattern across Europe, however, depends strongly on the season and index we look at. The hottest summer daytime temperature extremes (TXx) and tropical nights (TR) increase predominately in the Mediterranean region, whereas the coldest winter nighttime temperature extremes (TNn) increase in Central and Northern Europe with highest rates in northeastern Europe. In CLE$_{mod}$ and GHG, similar patterns of changes in TNn and TR are evident. This is not the case for TXx, for which we see significant increases particularly in northern parts of Europe in CLE$_{mod}$ but only small or no changes in GHG.

[16] Changes in the precipitation extremes, represented by the RX5d, R95p, and CDD indices, can be seen in parts of Europe in Figure 2; however, the areas with significant changes are substantially reduced compared to the temperature extremes. The strongest changes can again be seen in MFR with increases in the wet extremes across central and northern parts for RX5d and increases particularly in northern parts of Europe for R95p. Increases in the dry extremes (CDD) are concentrated around the Mediterranean region. In the CLE$_{mod}$ and GHG scenario,

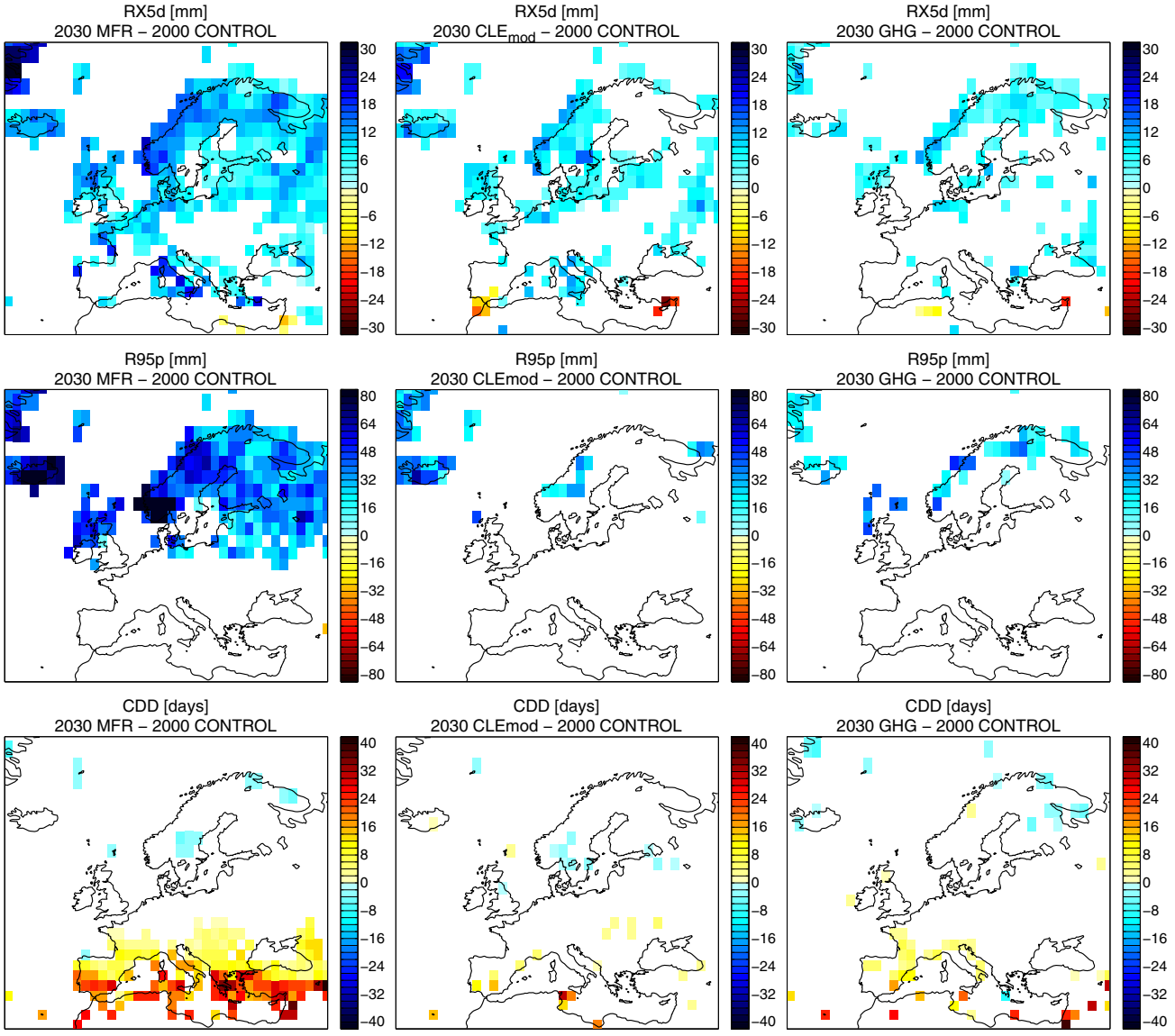

Figure 2. Changes in extreme precipitation indices (RX5d, R95p, and CDD) due to the three future scenarios, maximum feasible reduction (MFR, left panels), MFR in Europe only and current legislation emission in the rest of the world (CLE_{mod}, middle panels), and GHG only emission scenario (GHG, right panels), compared to present climate conditions (CONTROL). Ocean grid cells and changes not statistically significant at the 5% significance level are not shown.

a coherent pattern of increase can be seen particularly for RX5d, mainly in northern Europe, whereas only scattered grid boxes indicate significant changes in R95p and CDD across Europe.

3.2. Regional Quantification of Changes

[17] The differences between future and present climate simulations for three European regions are plotted in Figure 3, which indicates an average increase of TXx (Figure 3a) in MFR by about 4.1°C, 3.6°C, and 2.6°C in the Mediterranean region (MED), Central Europe (CEU), and Northern Europe (NEU), respectively. This north-south gradient occurs also in the GHG scenario but with smaller differences between the regions ranging from 1.6°C in MED to 1.2°C in NEU. Increases of TXx in CLE_{mod} are very similar across the regions and range around 1.9°C. This gradient is also reflected in TR (Figure 3b) with largest increases in MED (55 days) and smallest in NEU within 2 days. Note, however, that TR are already very rare under present climate conditions in Northern Europe. We can see more TR (25 days) in CLE_{mod} than in GHG (21 days) in MED and much less in CEU (5–6 days). The north-south gradient is reversed for TNn (Figure 3c), where we see the strongest increase in the MFR scenario in NEU (7.9°C) followed by CEU (7°C) and the least in MED (4.3°C). Interestingly, the differences between the CLE_{mod} and GHG scenarios for TNn are very small in the three regions, with increases of about 2°C in MED, ≈4°C in CEU, and 4.7°C in NEU.

[18] For the precipitation extremes, RX5d and R95p (Figures 3d and 3e), we can also see a north-south gradient with small changes in the MED and largest changes in NEU. RX5d increases by 9.5 mm in NEU, 6.5 mm in CEU, and 4.3 mm in MED in the MFR scenario. Changes in

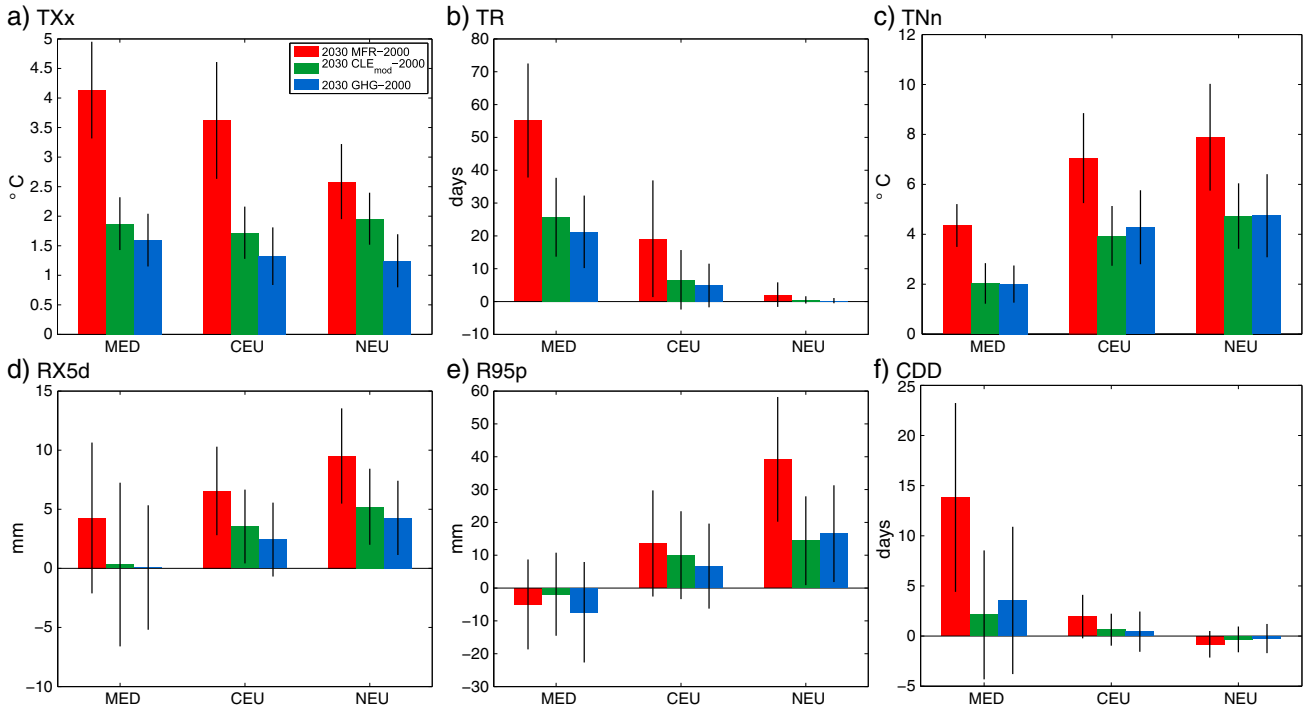

Figure 3. Average differences over Europe (Mediterranean region [MED; 12°W–40°E, 35°N–45°N], Central Europe [CEU; 12°W–40°E, 45°N–55°N], Northern Europe [NEU; 12°W–40°E, 55°N–70°N]) between three future scenarios (GHG, MFR, and CLE_{mod}) and the CONTROL simulation for year 2000 with extreme temperature indices (TXx, TR, and TNn) and extreme precipitation indices (RX5d, R95p, and CDD). Vertical bars indicate the ±1 standard deviation of regional differences derived from three ensemble simulations of each scenario. The mean values for each region from the year 2000 CONTROL simulation are provided in Table S3 of the supporting information.

CLE_{mod} and GHG are close to 0 in MED, 2.4 and 3.5 mm, respectively, in CEU, and 4.2 and 5.2 mm in NEU. Larger differentiation between the regions can be found for R95p particularly for MFR, where we see a small decrease in MED and increases of 13.6 mm in CEU and 39.2 mm in NEU. The changes in CLE_{mod} and GHG are 16.6 and 14.4 mm in NEU, which is about half of the change projected for MFR. Extreme dry conditions, as represented by CDD (Figure 3f), increase strongest in MED with ≈14 days in MFR and only about 2–3 days in CLE_{mod} and GHG, respectively. The changes are close to 0 and insignificant for the other regions in all scenarios.

4. Discussion and Conclusion

[19] We have shown that a global reduction of aerosols (i.e., sulfate and black and organic carbon) can greatly enforce the global warming effect due to greenhouse gases. The patterns of changes in extremes over Europe as simulated in the maximum feasible reduction scenario (MFR) for the year 2030 resemble closely the patterns projected for the end of the 21st century (cf. Figures 5 and 7 in *Sillmann and Roeckner* [2008]) in two SRES scenarios. This is an increase in the hottest summer daytime temperatures (TXx), tropical nights (TR), and consecutive dry days (CDD) over southern parts of Europe and a strong increase in the coldest winter nighttime temperatures and extreme precipitation magnitudes (RX5d and R95p) particularly over northern parts of Europe.

[20] If a maximum feasible aerosol reduction is only implemented over Europe and the rest of the world is following the current legislation scenario (CLE_{mod}), regional effects of aerosol forcings can be distinguished. As the regional cooling effect of aerosols is most efficient during summer months when incoming solar radiation is scattered most efficiently by the aerosols, their reduction will cause a stronger regional heating and, thus, result in hotter daily temperature extremes. This becomes most obvious in the increase of TXx in Northern Europe, which is more pronounced in CLE_{mod} than in the GHG scenario. There seems to be no distinguishable effect of regional aerosol forcing on the coldest winter nights (TNn) and tropical nights (TR) nor on the precipitation extremes. Further studies are needed to explain these regional features, which may also be associated with nonlinear aerosol indirect effects and changes in atmospheric circulation and clouds in response to changes in emissions.

[21] Note that the results discussed in this paper are based on simulations of only one climate model. We strongly encourage coordinated multimodel simulations of aerosol scenarios as discussed in this study to be able to carefully assess model-related uncertainties, which are also important for the quantification of the aerosol effect on climate extremes.

[22] To conclude, the changes in temperature and precipitation extremes as projected in anthropogenic climate change scenarios (i.e., SRES scenarios) will be magnified strongly if aerosol emissions are reduced globally. Thus,

concomitant with the aerosol reductions, there has to be a reduction of greenhouse gas concentrations to mitigate climate change. A reduction of aerosols that does not exacerbate global warming could be obtained, for instance, with measures mainly targeted at reducing absorbing particles such as black carbon. Aerosols and greenhouse gases, however, act on different time scales: Due to their relatively short atmospheric lifetime (on the order of about a week for tropospheric aerosols), reductions in aerosol emissions have more rapid effects on climate than longer-lived greenhouse gases.

[23] This paper illustrates that the effect of aerosols on climate extremes deserves much more attention when discussing future aerosol emission regulations on national and international levels. Concomitantly, it needs much more attention in future research studies involving, for instance, multimodel simulations of complex Earth system models to account for model-related uncertainties and relevant feedback mechanisms between the interacting climate system components.

[24] **Acknowledgments.** The work of J. Sillmann is supported by a grant (Si 1659/1-1) from the German Research Foundation (DFG). The authors thank Knut von Salzen and one anonymous reviewer for their helpful comments on the manuscript.

[25] The Editor thanks an anonymous reviewer for his/her assistance in evaluating this paper.

References

Caesar, J., and J. A. Lowe (2012), Comparing the impacts of mitigation versus non-intervention scenarios on future temperature and precipitation extremes in the HadGEM2 climate model, *J. Geophys. Res.*, *117*, D15109, doi:10.1029/2012JD017762.

Cofala, J., M. Amann, Z. Klimont, K. Kupiainen, and L. Höglund-Isaksson (2007), Scenarios of global anthropogenic emissions of air pollutants and methane until 2030, *Atmos. Environ.*, *41*, 8486–8499.

Feichter, J., E. Kjellstrom, H. Rodhe, F. Dentener, J. Lelieveld, and G. Roelofs (1996), Simulation of the tropospheric sulfur cycle in a global climate model, *Atmos. Environ.*, 30, 1693–1707.

Fiore, A. M., et al. (2012), Global air quality and climate, *Chem. Soc. Rev.*, *41*, 6663–6683.

Forster, P., et al. (2007), *Climate Change 2007: The Physical Science Basis. Contribution of Working Group I to the Fourth Assessment Report of the Intergovernmental Panel on Climate Change*, pp. 130–234, chap. Changes in Atmospheric Constituents and in Radiative Forcing, Cambridge University Press, Cambridge, United Kingdom and New York, NY, USA.

Kloster, S., F. Dentener, J. Feichter, F. Raes, U. Lohmann, E. Roeckner, and I. Fischer-Bruns (2010), A GCM study of future climate response to aerosol pollution reductions, *Clim. Dynam.*, *34*, 1177–1194.

Kulmala, M., et al. (2011), General overview: European Integrated project on Aerosol Cloud Climate and Air Quality Interactions (EUCAARI)—Integrating aerosol research from nano to global scales, *Atmos. Chem. Phys.*, *11*, 13,061–130,143.

Nakicenovic, N., et al. (2000), *Special Report on Emission Scenarios*, 612 pp., Cambridge University Press, Cambridge, UK. ISBN 0521804930.

Orlowsky, B., and S. I. Seneviratne (2012), Global changes in extreme events: Regional and seasonal dimension, *Clim. Change*, *110*, 669–696.

Patz, J. A., D. Campbell-Lendrum, T. Holloway, and J. A. Foley (2005), Impact of regional climate change on human health, *Nat. Rev.*, *438*, 310–317.

Ramanathan, V., and Y. Feng (2009), Air pollution, greenhouse gases and climate change: Global and regional perspectives, *Atmos. Environ.*, *43*, 37–50.

Roeckner, E., T. Siebert, and J. Feichter (1995), Climatic response to anthropogenic sulfate forcing simulated with a general circulation model, in *Proceedings of the Dahlem Workshop on Aerosol Forcing of Climate*, edited by R. J. Charlson and J. Heintzenberg, John Wiley & Sons, Chichester.

Roeckner, E., et al. (2003), The atmospheric general circulation model ECHAM5. Part 1: Model description, *MPI Report 349*, Max Planck Institute for Meteorology.

IPCC (2012), *Managing the Risks of Extreme Events and Disasters to Advance Climate Change Adaptation. A Special Report of Working Groups I and II of the Intergovernmental Panel on Climate Change*, 582 pp., Cambridge University Press, Cambridge, UK, and New York, NY, USA.

Sillmann, J., and E. Roeckner (2008), Indices for extreme climate events in projections of anthropogenic climate change, *Clim. Change*, *86*, 83–104.

Sillmann, J., V. V. Kharin, X. Zhang, F. W. Zwiers, and D. Bronaugh (2013a), Climate extremes indices in the CMIP5 multimodel ensemble: Part 1. Model evaluation in the present climate, *J. Geophys. Res. Atmos.*, *118*, 1716–1733, doi:10.1002/jgrd.50203.

Sillmann, J., V. V. Kharin, F. W. Zwiers, X. Zhang, and D. Bronaugh (2013b), Climate extremes indices in the CMIP5 multimodel ensemble: Part 2. Future climate projections, *J. Geophys. Res. Atmos.*, *118*, 2473–2493, doi:10.1002/jgrd.50188.

Stier, P., et al. (2005), The aerosol-climate model ECHAM5-HAM, *Atmos. Chem. Phys.*, *5*, 1125–1156.

Tebaldi, C., K. Hayhoe, J. Arblaster, and G. Meehl (2006), Going to extremes: An intercomparison of model-simulated historical and future changes in extreme events, *Clim. Change*, *79*, 185–211.

Vignati, E., J. Wilson, and P. Stier (2004), M7: An efficient size-resolved aerosol microphysics module for large-scale aerosol transport models, *J. Geophys. Res.*, *109*, D22202, doi:10.1029/2003JD004485.

Zhang, X., L. Alexander, G. C. Hegerl, P. Jones, A. K. Tank, T. C. Peterson, B. Trewin, and F. W. Zwiers (2011), Indices for monitoring changes in extremes based on daily temperature and precipitation data, *WIREs Clim. Change*, *2*, 851–870.